The Radius of Gyration of Native and Reductively Methylated Myosin Subfragment-1 from Neutron Scattering

Deborah B. Stone,* Dieter K. Schneider,‡ Ziwei Huang,§ and Robert A. Mendelson*
*Cardiovascular Research Institute and Department of Biochemistry and Biophysics, and §Department of Pharmaceutical Chemistry, University of California, San Francisco, California 94143; and ‡Biology Department, Brookhaven National Laboratory, Upton, New York 11973.

ABSTRACT Reductive methylation of nearly all lysine groups of myosin subfragment-1 (S1) was required for crystallization and solution of its structure at atomic resolution. Possible effects of such methylation on the radius of gyration of chicken skeletal muscle myosin S1 have been investigated by using small-angle neutron scattering. In addition, we have investigated the effect of MgADP·V_i, which is thought to produce an analog of the S1·ADP·P_i state, on the S1 radius of gyration. We find that although methylation of S1, with or without SO_4^{2-} ion addition, does not significantly alter the structure, addition of ADP plus vanadate does decrease the radius of gyration significantly. The S1 crystal structure predicts a radius of gyration close to that measured here by neutron scattering. These results suggest that the overall shape found by crystallography resembles nucleotide-free S1 in solution. In order to estimate the effect of residues missing from the crystal structure, the structure of missing loops was estimated by secondary-structure prediction methods. Calculations using the complete crystal structure show that a simple closure of the nucleotide cleft by a rigid-body torsional rotation of residues (172–180 to 670) around an axis running along the base of the cleft alone does not produce changes as large as seen here and in x-ray scattering results. On the other hand, a rigid body rotation of either the light-chain binding domain (767 to 843 plus light chains) or of a portion of 20-kDa peptide plus this domain (706 to 843 plus light chains) is more readily capable of producing such changes.

INTRODUCTION

Myosin is a Y-shaped molecule containing a long coiled-coil rod and two globular elongate heads. Each of these 130-kDa globular "motor domains" contains ATP and actin binding sites and two light chains. It has been demonstrated that proteolytically isolated heads, termed subfragment-1 (S1), are capable of supporting sliding movement of actin in the presence of ATP (Toyoshima et al., 1987). The recent solution of the crystal structure of S1 (Rayment et al., 1993a) now provides an important framework on which an understanding of the molecular events of contraction can be built.

In order to achieve crystals suitable for analysis, it was necessary to modify S1 by reductive methylation leading to dimethylation of nearly all of the 103 lysine ϵ-NH_2 groups. Although a parallel study on lysozyme (Rypniewski et al., 1993) showed that reductive methylation of all six lysine residues of that protein resulted in very little perturbation of its atomic structure, it is not certain that such a conclusion can also be drawn for the S1 portion of myosin. After reductive methylation, lysozyme retains nearly full catalytic activity (Fretheim et al., 1979) while S1 displays marked changes in enzymatic activity (White and Rayment, 1993) similar to those resulting from other modifications that have been linked to (local) conformational changes in S1 (Bivin et al., 1994). Furthermore, methylation of the lysine residues of alcohol dehydrogenase increased both enzyme activity and heat stability and resulted in changes in the ultraviolet and optical rotatory dispersion spectra and elution pattern from Sephadex G-100, indicative of major conformational changes in the protein (Tsai et al., 1974). In the present study, small-angle neutron scattering from native and reductively methylated myosin S1 (RM-S1) in solution has been carried out to search for any large-scale alterations in structure due to the lysine modification. We have also compared the scattering of methylated S1 bearing an SO_4^{2-} ion in the active site with that of native S1. Because this ion was bound in crystals of methylated S1 that were used to determine the S1 structure (Rayment et al., 1993a), it is also possible that these two alterations could synergistically make large-scale changes in S1 structure.

In addition to directly studying the specific effect of methylation on the radius of gyration (R_g), we also compared the observed R_g of S1 with that predicted by the Rayment et al. (1993a) crystal structure. This provides an additional test of the effect of methylation and also explores whether there are any large-scale deformations that might be induced upon crystallization. Such effects might be expected inasmuch as there have been reports (Vibert and Cohen, 1988; Rayment et al., 1993b) of possible flexibility in the light-chain binding region of S1, which consists of a long, single α-helix surrounded by the two light chains. There have been small but potentially important differences between the R_g values reported by different laboratories (Mendelson et al., 1991; Garrigos et al., 1992; Wakabayashi et al., 1992), which need to be explored before such a comparison can be meaningfully undertaken.

Received for publication 1 March 1995 and in final form 25 May 1995.

Address reprint requests to Dr. Robert A. Mendelson, Cardiovascular Research Institute and Department of Biochemistry and Biophysics, University of California, San Francisco, CA 94143-0524. Tel.: 415-476-1827; Fax: 415-476-8173; E-mail: mendel@musl.ucsf.edu.

0006-3495/95/09/767/10 $2.00

Because the decrease in R_g observed during ATP hydrolysis has been taken as support for the model of muscle contraction suggested by Rayment et al. (1993b), we have also investigated the effect of adding ADP and vanadate to S1 by using neutron scattering [as has been done by Wakabayashi et al. (1992) using x-ray scattering]. Because S1·ADP·V_i is regarded as an analog of S1·ADP·P_i, the predominant steady-state intermediate of myosin ATPase (Goodno and Taylor, 1982), it might be expected to produce an S1 structural change similar to that observed when ATP is undergoing steady-state hydrolysis by S1.

Neutron scattering is a useful tool for these studies because neutrons produce far less radiation damage to the sample than do x-rays (Schoenborn, 1975). Thus, in contrast to x-ray scattering, one can add nucleotide to a previously exposed sample and perform accurate difference measurements. Also, when experiments are performed in D_2O buffers, the intrinsic high scattering contrast and low solvent background allow reliable measurements of the apparent R_g at lower protein concentrations than are possible with x-rays.

MATERIALS AND METHODS

Proteins

Myosin was isolated from adult chicken pectoralis muscle and digested with papain in the presence of $MgCl_2$ by the method of Margossian and Lowey (1982), with the following modifications. In order to minimize light chain-2 (LC2) proteolysis and polydispersity in heavy-chain proteolysis, the digestion of myosin was carried out for 10 min at 22°C with a papain to myosin ratio of 1:1333. The resulting S1 yield was 15–30% of the theoretical maximum. The S1 in the digest supernatant was purified by anion exchange chromatography on Q Sepharose fast flow, Q Sepharose HP (Pharmacia, Piscataway, NJ) or QHR8 (Waters, Milford, MA) followed by size exclusion chromatography on either an 80-cm S200-HR or a 30-cm Superdex 200-HR high performance column (Pharmacia). The solvent for all columns was 50 mM imidazole (pH 7), 0.5 mM $MgCl_2$, 1 mM dithiothreitol (DTT) with the addition of a 100–400 mM NaCl gradient for Q Sepharose, a 0–200 mM NaCl gradient for QHR8 (Waters), and 100 mM NaCl for size exclusion columns.

The lysine residues of the purified S1 were reductively methylated by reaction with dimethylamine borane complex (Aldrich Chemical Co., Milwaukee, WI) and methanol-free formaldehyde (Electron Microscopy Sciences, Fort Washington, PA), as described by Rayment et al. (1993a) and White and Rayment (1993). The reaction was terminated by the addition of ammonium sulfate to 75% saturation (Rypniewski et al., 1993), and the precipitated protein was collected by centrifugation and dialyzed before lyophilization in the presence of sucrose (Takashi et al., 1982). The degree of modification was determined by amino acid analysis (at the Protein and Nucleic Acid Facility, Stanford University Medical Center, Stanford, CA) on samples that had been exhaustively dialyzed against N-ethylmorpholine-acetate, pH 8 (Rypniewski et al., 1993). Before data acquisition, samples of lyophilized native and methylated S1 were usually further purified on a fast protein liquid chromatography size-exclusion column (Superdex 200-HR). Column fractions to be analyzed by neutron scattering were dialyzed overnight at 6°C against a 99% D_2O solvent containing 50 mM imidazole (pH 7.5), 110 mM KCl, 1 mM $MgCl_2$, 0.2 mM DTT, 0.1 mM NaN_3, and protease inhibitors, and in most instances they were clarified at 120,000 × g for 45–60 min.

In one set of experiments, Na_2SO_4 in D_2O was added directly to methylated S1 solutions to a final concentration of 45 mM along with an additional 3 mM $MgCl_2$. Sulfate binding at the S1 active site under these conditions has been demonstrated by quenching of fluorescein-labeled S1 (Aguirre et al., 1986), competitive inhibition of ϵ-ATP binding (Tesi et al., 1988), and release of V_i from S1·MgADP·V_i complex (Muhlrad et al., 1991).

S1·ADP·V_i was prepared by the method of Goodno (1982) using final concentrations of 0.5 mM ADP and 0.5 mM Na_3VO_4 to avoid formation of polymeric species of V_i (Smith and Eisenberg, 1990). Measurement of MgATPase activity indicated nearly complete inhibition of this activity by formation of the S1·ADP·V_i complex.

ATPase measurements were carried out by the method of White (1982). Actin was prepared from rabbit skeletal muscle by the method of Spudich and Watt (1971).

Small-angle neutron scattering

Neutron scattering measurements were performed at the H9B beamline on the High Flux Beam Reactor at Brookhaven National Laboratory (BNL) and at the NG3 beamline at the Cold Neutron Research Facility at the National Institute of Standards and Technology (NIST). At BNL, the neutron wavelength (λ) was 0.73 nm with a full width at half maximum spread of $\Delta\lambda/\lambda = 0.12$. The sample-to-detector distance was 1.75 m and the beam diameter was 0.6 cm. At NIST, two geometries were employed: one with $\lambda = 0.55$ nm, $\Delta\lambda/\lambda = 0.15$, a sample-to-detector distance of 5 m with a 20-cm offset and the other with $\lambda = 0.55$ nm, $\Delta\lambda/\lambda = 0.34$ and a sample-to-detector distance of 9.0 m. At BNL, the wavelength was calibrated by using the (001) powder diffraction of silver beneate and at NIST by time-of-flight measurements and secondarily by silver beneate. At BNL and NIST, solutions were contained in standard quartz spectrophotometer cells with path lengths of 2 and 5 mm. In addition, large cylindrical cells having a 5-mm path length were sometimes used at NIST to allow full utilization of the 1.6-cm diameter beam. Absolute intensity calibrations and detector efficiency corrections were performed by using a 1-mm thick H_2O sample. Sample exposures were 0.5–4.0 h. All experiments were performed at 6°C. Data were analyzed using the program SCATMAN, which propagates the statistical error arising in each detector pixel.

Calculation of the scattering intensity expected from the crystal structure

The Debye equation was used to compute the scattering curve from the crystallographically determined structure of S1. Each amino acid was represented by a sphere positioned at the C_α position. The true amino acid volumes and scattering lengths (Σb_i) were obtained from Jacrot and Zaccai (1981). Tests using other crystallographically determined structures having complete atomic coordinates available showed that this approach was adequate to accurately compute scattering curves at the resolution typical of solution scattering experiments ($s < 1/2.5$ nm^{-1}).

When comparing the measured R_g with the in vacuo R_g computed from the crystallographically determined structure, it is necessary to account for deviations caused by scattering-length density fluctuations. This was done by means of the Stuhrmann equation (e.g. Ibel and Stuhrmann, 1979):

$$R_g^2 = R_c^2 + \alpha/\Delta\rho - \beta/(\Delta\rho)^2. \quad (1)$$

Here R_g is the measured R_g, which is a function of contrast. The scattering contrast, $\Delta\rho$, is the difference between the average solute scattering-length density $\langle\rho_{pro}\rangle$ and that of the solvent, ρ_{sol}. R_c is the R_g at infinite contrast, i.e., that of the shape of S1, and α and β are first and second moments of the scattering density fluctuations about $\langle\rho_{pro}\rangle$. For neutron scattering from samples in 8% D_2O buffers, the solvent scattering length vanishes, and $R_g^{\text{in vacuo}}$, which can be compared directly with crystallographic results, is obtained. (Note that the high incoherent background scattering by H_2O makes accurate experiments in 8% D_2O at low protein concentrations infeasible). Using Eq. 1, the R_g measured in a buffer having any D_2O content is

$$R_g = \left[(R_g^{\text{in vacuo}})^2 + \alpha\left(\frac{1}{\Delta\rho} - \frac{1}{\langle\rho_{pro}\rangle}\right) - \beta\left(\frac{1}{\Delta\rho^2} - \frac{1}{\langle\rho_{pro}\rangle^2}\right)\right]^{1/2}. \quad (2)$$

Thus, the expected R_gs in 100% D_2O were computed by using known scattering length densities and α, β, and $R_g^{\text{in vacuo}}$, which were computed from the crystallographic C_α-map from the Protein Data Bank file *1mys*.

In a real experiment, the measured effective R_g at concentration c, $R_g^{\text{eff}}(c)$, can deviate from the expected $R_g(c)$ due to experimental limitations, which prevent measurements at the very smallest scattering angles. In order to compute $R_g^{\text{eff}}(0)$ from the crystal structure, a numerical simulation was used. Poisson-distributed noise was appropriately folded with the computed intensity curve, which had the approximate statistical accuracy of a typical experiment. Straight-line least-squares fits to a model Guinier plot [ln I(s) vs. s^2] were then made in the s^2 range of interest to extract the model $R_g^{\text{eff}}(0)$. It was found that the effect of finite statistical accuracy on the prediction of $R_g^{\text{eff}}(0)$ was negligible in the s^2 ranges considered.

In order to estimate the true R_g of the intact molecule, the structures of missing residues were estimated. This was accomplished in the following manner. The full atom coordinates of S1 were generated on the basis of the available C_α positions with software Discover/Insight II (Biosym Technologies, San Diego, CA). The computational program BLOOP (Huang et al., 1994; Ring et al., 1992) was used to generate plausible conformations for loops that are missed in the x-ray structure of S1. For incomplete COOH— and NH_2—termini, the appropriate residues were inserted with the coordinates of the last (first) known terminal residue.

RESULTS

Preparation of S1

Initial experiments analyzed the relationship between the method of purification and the measured $R_g^{\text{eff}}(c)$ of S1. The central portion of a Q Sepharose protein peak (containing S1 largely devoid of contaminants and enzymatically clipped LC2) was concentrated and applied to an S200-HR gel filtration column. Fig. 1 *a* shows a sodium dodecyl sulfate (SDS) gel of the S200-HR column fractions. In fraction 30, a small amount of high molecular weight contamination (probably a piece of myosin rod) that runs behind the intact S1 heavy-chain band is seen. Fractions 30, 32, and 34 were dialyzed against the D_2O-containing solvent and analyzed by neutron scattering. Guinier plots are shown in Fig. 1 *b*. S200-HR fractions 32 and 34, which were essentially devoid of high molecular weight contaminants, produced linear Guinier plots with lower R_g values. S200-HR fraction 30, which contained some high molecular weight contaminants (Fig. 1 *a*), yielded a Guinier plot of steeper slope and larger R_g. S200-HR fractions 32–34 were pooled and lyophilized. When this material was dissolved in D_2O buffer, the measured $R_g^{\text{eff}}(c)$ increased slightly, even after clarification. However, passage through a Superdex size-exclusion column produced peak fractions having $R_g^{\text{eff}}(c)$ values of 4.3–4.4 nm, comparable with those obtained from freshly prepared S1.

Subsequent preparations of S1 were either freshly prepared from myosin or lyophilized after anion exchange chromatography (with or without size exclusion chromatography) and purified by size exclusion chromatography immediately before data acquisition [a procedure comparable with that employed by Garrigos et al. (1992)]. High molecular weight contaminants were avoided, and an enrichment in S1-LC3 was obtained by taking suitable central fractions from conventional or high performance Q-columns. However, although a detailed study was not undertaken, we found no significant difference in R_gs between samples with varying enrichments of LC3. A typical gel of such S1 and also of methylated S1 is shown in Fig. 1 *c*.

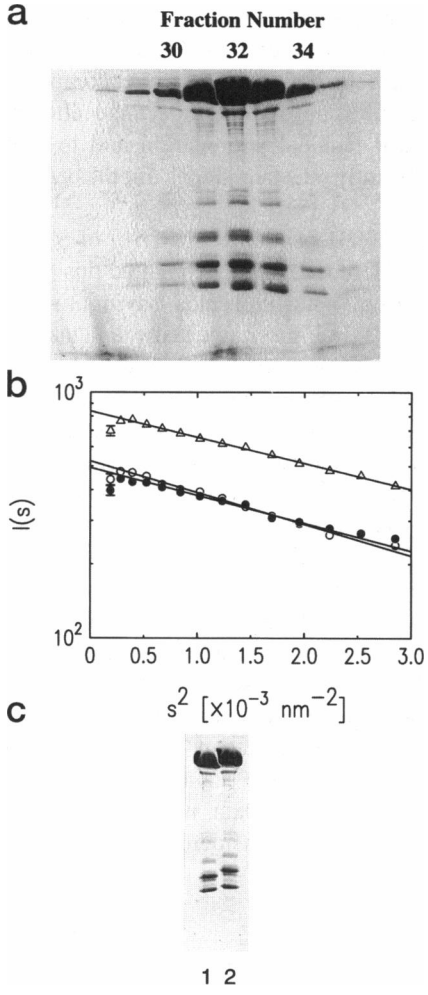

FIGURE 1 (*a*) 15% Polyacrylamide gel electrophoresis-SDS of column fractions from an S200-HR gel filtration column; (*b*) Guinier plots for S200-HR column fractions. $R_g^{\text{eff}}s$ for fractions 30 (○), 32 (△), and 34 (●) are 4.76 ± 0.14 nm, 4.39 ± 0.09 nm, and 4.50 ± 0.14 nm, respectively. The protein concentrations of fractions 30, 32, and 34 were 0.58, 0.83, and 0.46 mg/ml, respectively. The solid lines are straight line least-squares fits over the range of $s^2 = 0.778 \times 10^{-3}$ to $s^2 = 2.22 \times 10^{-3}$ nm^{-2}. (*c*) 15% Polyacrylamide gel electrophoresis-SDS of native S1 (*lane 1*) and methylated S1 (*lane 2*).

The R_g of S1

Here we have analyzed the R_g over the same s^2 range as that employed by Wakabayashi et al. (1992) ($s^2 = 0.778$–2.22×10^{-3} nm^{-2}). As will be discussed later, this range, and to a lesser extent the somewhat lower range of s^2 employed by Garrigos et al. (1992), yielded an $R_g^{\text{eff}}(0)$ that is somewhat smaller than the in vacuo R_g calculated from the S1 structure (Rayment et al., 1993a). Nevertheless, the range used by Wakabayashi et al. (1992) has been employed in this

work because it minimizes the effect of any residual aggregation and minimizes concentration dependence due to excluded volume effects; it also allows direct comparison with their results. In addition, use of this range allowed us to assay samples for residual aggregation and to reject data that had significantly steeper slopes in the very low s^2-range.

The concentration dependence of $R_g^{eff}(c)$ of S1 in D_2O is shown in Fig. 2. Here we have investigated this dependence by using data from neutron beams having two different wavelength spreads. In Fig. 2 *a*, we show data taken at NIST with $\Delta\lambda/\lambda = 0.34$. [Convolution of the calculated S1 scattering curve with this wavelength spread and with the experimental apertures did not produce a significant decrease in $R_g^{eff}(0)$ from the ideal (unconvolved) value.] The use of $\Delta\lambda/\lambda = 0.34$ produces a concentration plot with high statistical accuracy at the expense of increasing the uncertainty in the absolute $R_g^{eff}(0)$. This is because the larger wavelength spread somewhat increases the uncertainty in the determination of the mean wavelength. Note that the slight concentration dependence seen in the $\Delta\lambda/\lambda = 0.34$ data seems to be significantly less than that seen by Wakabayashi et al. (1992). Here the slope of our concentration plot is outside of two standard deviations of that of Wakabayashi et al. (although we do not know the standard deviation of their slope). If $\Delta\lambda/\lambda = 0.12$–$0.15$ data, or all data weighted only by statistical accuracy are considered (Fig. 2 *b*), the deviation of the concentration dependence from that of Wakabayashi et al. (1992) is even greater. We find that the $R_g^{eff}(0)$ in D_2O is 4.41 ± 0.07 nm. This was determined by using data taken primarily with $\Delta\lambda/\lambda = 0.12$–$0.15$ (Fig. 2 *b*). Absolute measurements using water and assuming a partial specific volume of 0.73 ml/g yielded an observed molecular weight that is within 15% of the actual molecular weight. This indicates that aggregation was not distorting our data to a significant degree.

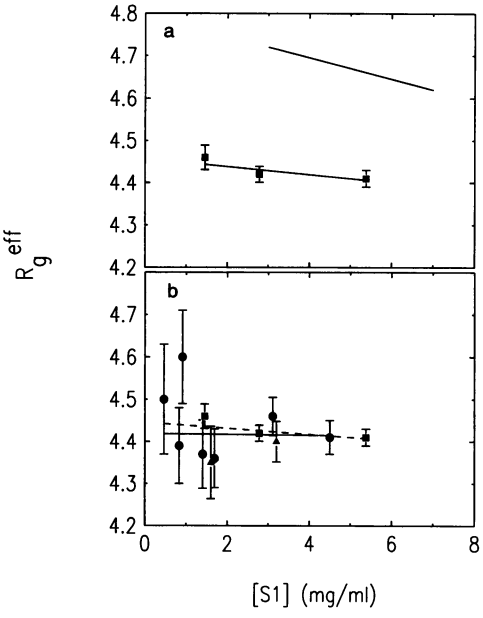

FIGURE 2 Concentration dependence of R_g^{eff}. (*a*) $R_g^{eff}(c)$ measured with $\Delta\lambda/\lambda = 0.34$ at NIST. Slope = −0.0095 ± 0.0081 nm/(mg/ml). Upper curve is the concentration dependence obtained from x-ray scattering by Wakabayashi et al. (1992) (slope = −0.025 nm/(mg/ml)). (*b*) $R_g^{eff}(c)$ determined with $\Delta\lambda/\lambda = 0.12$–$0.15$ data taken at BNL (●) and NIST (▲). Also included are $\Delta\lambda/\lambda = 0.34$ points (■) from (*a*). The solid straight line is a least-squares fit to points with $\Delta\lambda/\lambda = 0.12$–$0.15$ (slope = 0.0009 ± 0.016 nm/(mg/ml)), and the dashed line is a fit to all data points assuming statistical error only [slope = −0.007 ± 0.007 nm/(mg/ml)].

Effect of reductive methylation

Q Sepharose-purified S1 was reductively methylated by the procedure used by Rayment et al. (1993a). Amino acid analysis (Table 1) indicated that 98.2 (94%) of 104.8 lysine residues had been dimethylated on the ϵ-NH_2 group. The total number of lysine residues exclusive of Me_3Lys detected in the methylated sample (104.8) agreed with the number detected in native S1 (103.6), as well as the number predicted from the amino acid sequence. Rayment et al. (1993a) reported modification of 96.7 (96%) of 100.9 residues; however, there was greater discrepancy in the total number of lysine residues detected in native and methylated S1. No significant reduction of other amino acids was observed in the present study, indicating that modification was limited to the lysine residues. A gel of S1 and methylated S1, which are representative of material used in scattering studies and the amino acid analysis, is shown in Fig 1 *c*.

ATPase activities of native and methylated S1 are summarized in Table 2. The K^+(EDTA)-ATPase and the actin-

TABLE 1 Amino acid analysis of native and methylated myosin subfragment 1

	Rayment and White (1993)			Present work	
Amino acid	Theoretical	Native S1	RM-S1	Native S1	RM-S1
Aspartate + asparagine	114.5	118.9	119.2	117.4	117.0
Threonine	60	60.4	59.5	57.3	57.3
Serine	59	53.3	52.6	55.2	54.9
Glutamate + glutamine	153	161.6	161.4	166.0	165.4
Proline	48	51.2	50.5	48.8	49.5
Glycine	80	78.1	78.0	81.7	81.6
Alanine	91.5	86.0	85.4	87.3	85.3
Valine	66.5	67.1	66.9	63.4	63.4
Methionine	39	39.4	38.9	38.9	38.7
Isoleucine	69	60.7	60.9	59.3	59.8
Leucine	90.5	93.6	93.2	92.3	92.7
Tyrosine	37	40.4	40.2	38.0	37.9
Phenylalanine	72	74.1	73.9	71.5	72.9
Histidine	24	23.7	23.2	24.4	24.3
Arginine	46	47.5	47.2	47.7	47.6
Lysine	103	96.2	4.2	103.6	6.6
Me_1-Lys	0	0	0	0	0
Me_2-Lys	0	0.6	96.7	0	98.2
Me_3-Lys	3	3.6	3.4	3.0	3.0
Total lysine	106	100.4	104.3	106.6	107.8

TABLE 2 ATPase activity of native and methylated S1

Assay conditions	Native S1	Methylated S1
600 mM KCl, 5 mM EDTA, pH 8	6.04 s^{-1}	0.56 s^{-1}
600 mM KCl, 10 mM $CaCl_2$, pH 8	1.95 s^{-1}	5.04 s^{-1}
20 mM NaCl, 2 mM $MgCl_2$, pH 7.5	0.07 s^{-1}	0.33 s^{-1}
20 mM NaCl, actin-activated, V_{max}	10.1 s^{-1}	0.70 s^{-1}
20 mM NaCl, actin-activated, K_{app}	47 μM	38 μM

pH 8 assays contained 50 mM Tris, 1 mM DTT, and 5 mM ATP; pH 7.5 assays contained 10 mM HEPES, 1 mM DTT, and 1 mM ATP.

activated Mg^{++}-ATPase were inhibited ~90%, and the Ca^{2+}- and Mg^{++}-ATPase activities were elevated several-fold by reductive methylation. The apparent affinity of S1 for actin (K_{app}) was little changed by the modification. The Mg^{++}-ATPase activities are in agreement with those obtained by White and Rayment (1993) at a somewhat lower ionic strength where the actin-S1 affinity is enhanced. The pattern of inhibition of K^+(EDTA)-ATPase and activation of divalent cation-dependent ATPase agrees with that previously reported by Kitagawa et al. (1961) for reaction of a single lysyl ϵ-NH_2 group with 2,4,6-trinitrobenzenesulfonate and is typical of the effect of a number of myosin modifiers. The effect of methylation on ATPase activities reported here is also quite similar to several of those recently reported by Phan et al. (1994); however, because the latter authors did not carry out an amino acid analysis of the methylated protein, it is difficult to make a direct comparison.

When S1 [isolated from the central portion of the Q Sepharose peak (Fig. 3, *lane a*), not used for data acquisition] was stored on ice for a period of a month or more, significant proteolysis was observed (Fig. 3, *lane b*). However, S1 of the same preparation, which had been reductively methylated (Fig. 3, *lane c*), showed little proteolysis during the same period of storage (Fig. 3, *lane d*). Similar findings were obtained with a preparation of reductively methylated chymotryptic S1 (data not shown). In both cases, unreacted S1 was treated the same as reductively methylated S1, except for the addition of dimethylamine borane complex and formaldehyde. This will be discussed in greater detail later.

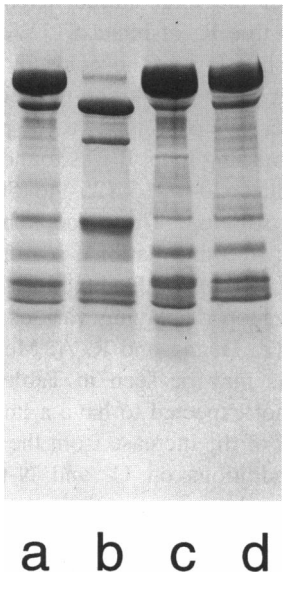

FIGURE 3 Gradient (4–20%) polyacrylamide gel electrophoresis-SDS of native and methylated papain-S1 before and after aging on ice for 1 month. Lane a, fresh native S1; lane b, aged native S1; lane c, fresh methylated S1; and lane d, aged methylated S1.

Guinier plots for native and methylated S1 at three protein concentrations are shown in Fig. 4. All methylated S1 scattering runs were made as difference measurements from an unmethylated control that had been purified and otherwise handled in the same manner before exposure. No significant difference in concentration dependence was observed (data not shown). The average percentage change in R_g due to methylation calculated for all of the data sets is $-0.4 \pm 0.9\%$. As seen in Tables 3 and 4, the crystal structure predicts that in the absence of large-scale conformational changes in the protein it is expected that the change in R_g due solely to methylation will indeed be quite small (-0.7%). Comparison of the scattering by methylated S1 with a sulfate ion in the active site with native S1 (with no additions) also showed no significant change in R_g. The lack of significant changes in R_g observed here indicates that any perturbations introduced by reductive methylation (and other similar modifiers) or methylation with a bound sulfate ion must indeed be local in nature.

Effect of ADP·vanadate addition to S1

$ADP{\cdot}V_i$ binding to S1 results in a small but definite decrease in R_g^{eff} (Table 3). Difference measurements were made using $\Delta\lambda/\lambda = 0.12$ and 0.34 at protein concentrations between 1.5 and 6 mg/ml. Here measurements were made on S1 control samples and then on the same samples with vanadate and ADP added. The fractional change in R_g^{eff} found here is within error of that found by Wakabayashi et al. (1992) using x-ray scattering and thus confirms their result. An approximate estimate of the sensitivity to such

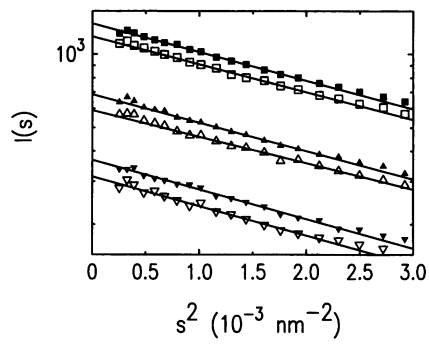

FIGURE 4 Guinier plots for native and methylated S1. Figure shows native S1: □, 3.1 mg/ml; Δ, 1.7 mg/ml; ▽, 0.85 mg/ml;and methylated S1: filled symbols at approximately the same concentrations. Solid lines are fits as in Fig. 1 *b*.

TABLE 3 Change in R_g^{eff} with additions to S1

Addition	[S1] range (mg/ml)	n*	$100\Delta R_g/R_g$ +SD (%)	Other results (%)
Methylation of lysines	0.8–6.0	8	−0.4 ± 0.9	−0.7‡
Methylation of lysines + SO_4^{2-}§	4.1–8.3	3	−1.1 ± 1.4	
ADP·V_i	1.5–6	4	−3.4 ± 1.1	−4 ± 1.3¶

*Abbreviations: n is the number of independent difference trials and $100\Delta R_g/R_g = 100[R_g\ (\text{addition}) - R_g\ (\text{control})]/R_g\ (\text{control})$. Exposures varied significantly between some trials.

‡Predictions based on the methylation of all lysine residues in the Rayment et al., (1993a) structure (see Table 4).

§In this instance it was assumed that the concentration dependence of R_g^{eff} with and without added SO_4^{2-} ion was identical.

¶Wakabayashi et al. (1992).

changes may be found in modeling studies (Wakabayashi et al., 1992; Garrigos et al., 1992) and will be discussed in more detail later.

Comparison with results from x-ray solution-scattering and crystallography

In order to examine whether the x-ray crystallographically determined structure of reductively methylated S1 is an accurate representation of native S1 in solution, we have made a comparison of our neutron scattering results and published x-ray solution scattering results with those predicted by this structure. In order to compare the measured $R_g^{eff}(0)$ with the true R_gs, a model scattering curve has been used to generate a Guinier plot (Fig. 5), which was then fit over either the s^2 range used by Garrigos et al. (1992) (region II) or the s^2 range used in our experiments and those of Wakabayashi et al. (1992) (region III). Fits over a very low s^2 range (region I) gave R_g values within 0.013 nm

TABLE 4 Comparison of measured S1 radii of gyration with crystallographic predictions

	Calculated				Experimental
	Rayment et al.		with added residues		
Parameter	S1	RM-S1	S1	RM-S1	S1*
In vacuo R_g (nm)	4.55	4.56	4.63–4.66	4.64–4.67	
X-rays‡					
R_g^{eff} (II)	4.39		4.47–4.50		4.67 ± 0.1§
R_g^{eff} (III)	4.34		4.41–4.44		4.78 ± 0.04¶
Neutrons					
R_g	4.41	4.38	4.47–4.49	4.42–4.44	
R_g^{eff} (III)	4.19	4.16	4.25–4.27	4.20–4.24	4.41 ± 0.07

*See Table 3 for results of neutron scattering by methylated S1.

‡Calculated x-ray R_g^{eff} predictions are presented, as is conventional, without contrast correction. Such corrections increase the computed R_g^{eff} by ~0.05 nm. Neutron predictions are corrected for contrast against the D_2O buffer using Eq. 2.

§Garrigos et al., 1992.

¶Wakabayashi et al., 1992

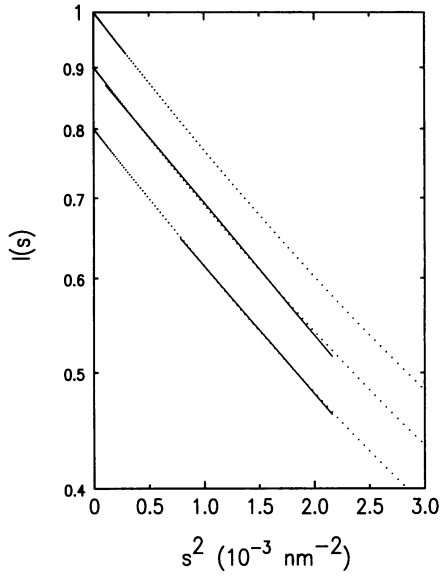

FIGURE 5 Guinier plots computed from the S1 structure of Rayment et al. (1993a) (····). The three fitting ranges shown from top to bottom correspond to the near-true Guinier region (I), the fitting range used by Garrigos et al. (1992) (II), and the fitting range used by Wakabayashi et al. (1992) (III) and in this work. The solid curves are least-squares fits of a straight line to the computed points (shown without simulated noise). The in vacuo R_g^{eff}s thus obtained are 4.54, 4.39, and 4.34 nm in regions I, II, and III, respectively. The true in vacuo R_g = 4.553 nm. Curves are arbitrarily normalized for display purposes.

(0.3%) of the true $R_g^{\text{in vacuo}}$ = 4.553 nm, computed directly from the charge or scattering-length distribution.

Table 4 summarizes the in vacuo R_gs, R_gs corrected for contrast using Eq. 2, and the $R_g^{eff}(0)$s experimentally expected. Because the Rayment et al. (1993a) crystal structure contains ~93% of the total amino acids, there is some uncertainly in the true R_g of intact S1. We have estimated the effect of the missing amino acids by completing the connectivity using secondary-structure prediction methods, as discussed earlier. We examined 18–20 plausible conformations for each missing loop. It was found that in all cases the loop at residues 204–216 (25- to 50-kDa junction) extends out into solution. These loops had qualitatively similar structures. A conformational search for the loop at residues 626–647 (50- to 20-kDa junction) indicated a large flexibility of this loop displaying various plausible structures in solution (Z. Huang and R. A. Mendelson, unpublished results). As may be seen in Table 4, the missing amino acids are not expected to have a large effect on the R_gs. Roughly half of the increase from the crystal structure R_g is due to readditions on C- and N-termini. Typical plausible loops are shown in Fig. 6 *a*.

All of the available data suggest that S1 in solution has a slightly larger R_g than that calculated by using the crystallographically determined structure (Table 4). Possible sources of this difference will be discussed later. Of the differences between crystallography and solution scattering, that of Wakabayashi et al. (1992) is the largest and most

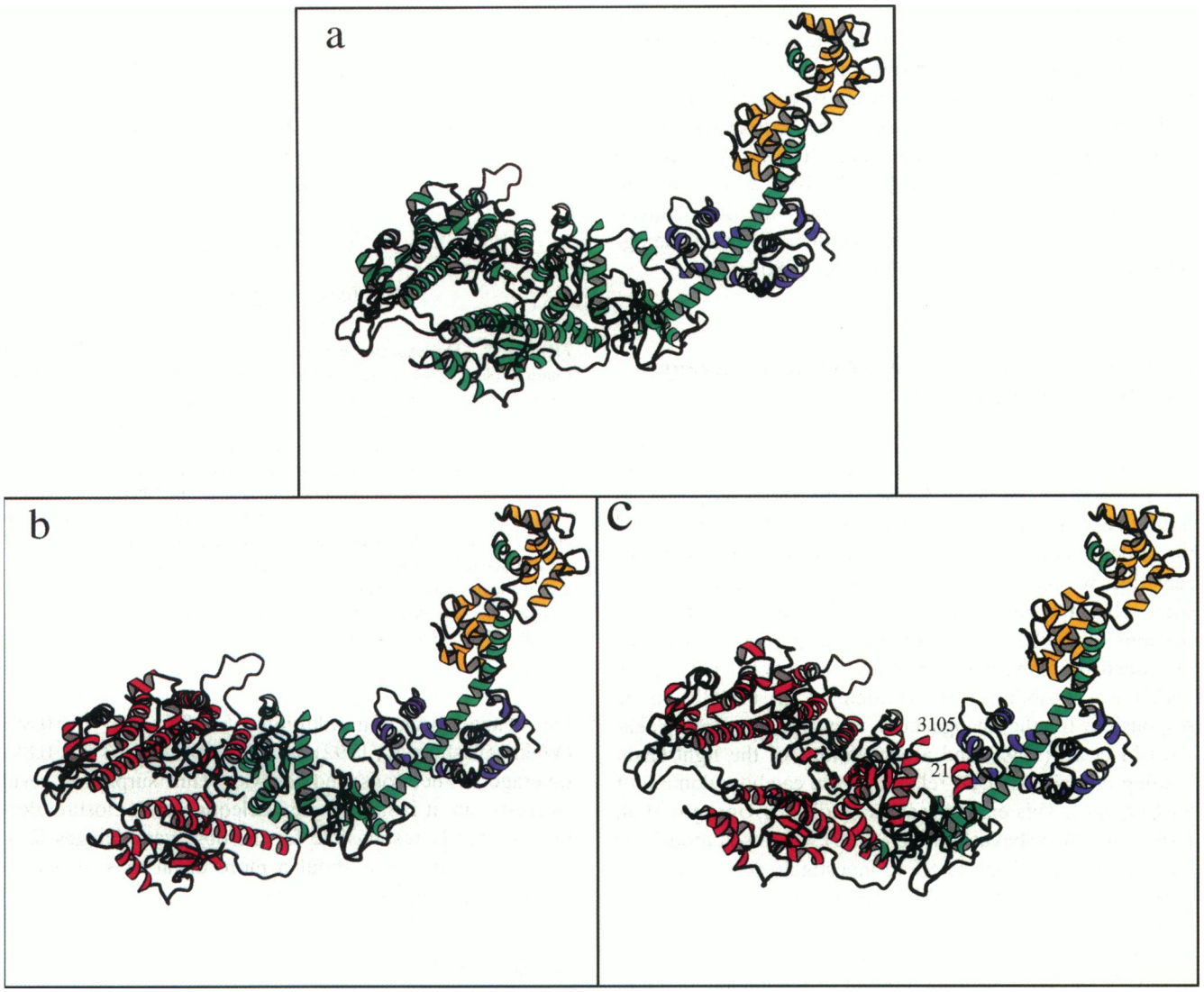

FIGURE 6 The structure of chicken myosin S1 (Rayment et al., 1993) and representative rigid-body rotations illustrating the two classes of distortions considered here. Figures were rendered using MOLSCRIPT (Kraulis, 1991). (*a*) The undistorted structure of S1 with missing loops added using the secondary structure prediction method discussed in the text; (*b*) a representative closure of the nucleotide cleft. Here residues 172–670 (red) were rotated about the 171–172 C_α-C_α chord relative to the remainder of the molecule. A +20° rotation is displayed here. (*c*) A representative bending of the LCBD relative to the main portion of S1. Here residues 1–705 (red) were rotated about the 705–706 C_α-C_α chord relative to the remainder of the molecule. A +20° rotation is displayed here. The position of residue 21 of the heavy chain and residue 105 of LC3 (denoted by 3105) are labeled here to show the position of putative heavy chain-light chain interaction. In parts *b* and *c* of this figure, the magnitudes of the changes have been exaggerated for display purposes. The position of the tail region of S1 has been held constant.

statistically significant. Note that if the Garrigos et al. (1992) data were fit over the same s^2 range as used here and by Wakabayashi et al. (1992) (region III), the Garrigos et al. (1992) R_g would decrease by about 0.06 nm to 4.61 ± 0.1 nm so that the disagreement between the two x-ray results exceeds one standard deviation and is statistically significant. Our S1 data do not show as great a concentration dependence of R_g^{eff} as found by Wakabayashi et al. (1992) and are perhaps more in agreement with the observations of Garrigos et al. (1992), which suggest that there is little or no concentration dependence. However, the concentration range used in the x-ray work of Garrigos et al. (1992) for papain-derived S1 was higher (8–14 mg/ml) than that used here (0.4–6 mg/ml) and thus was subject to greater uncertainty. The possibility exists that all or part of the difference between our concentration dependence and that of Wakabayashi et al. (1992) is caused by a real difference in the second virial coefficient of S1 due to experimental conditions (sample temperature, H_2O versus D_2O, etc.). This might not be demonstrated by the Garrigos et al. (1992) data because it does not go to concentrations as low as those used in the other experiments. However, in the absence of aggregation and sample polydispersity, the concentration dependence of R_g is caused by interparticle interference. Thus for a monodisperse solution it is to be expected that the concentration dependence in region II should be greater

than that in region III inasmuch as it extends to lower s^2. We note that the Garrigos et al. (1992) studies of chymotryptic S1, which lacks LC2, also showed no increase in $R_g^{eff}(c)$ as the concentration was lowered from 10 to 5 mg/ml.

The maximum chord predicted by the (anhydrous) crystal structure is in the 17–17.5 nm range. The x-ray scattering results of Wakabayashi et al. (1992) (16.7 ± 0.3 nm) and Garrigos et al. (1992) (19 ± 1.5 nm) are in adequate agreement with this value, given the difficulty of meaningfully deducing this parameter (Moore, 1980).

Modeling the sensitivity of solution scattering to structural changes in S1

In this and related studies, structural changes in S1 could arise when various nucleotides or nucleotide analogs bind to the active site or by methylation of the entire molecule. In order to obtain a more accurate estimate of the magnitude of the structural changes to which solution-scattering data are sensitive, we have computed changes in R_g on the basis of some plausible and representative rigid-body rotations of portions of the S1 crystal structure. In particular, we have examined the closure of the nucleotide pocket (Fig. 6 *b*), which was postulated by Rayment et al. (1993b) to be responsible for the change in R_g seen here and by Wakabayashi et al. (1992) and also rotations of the light-chain binding domain (LCBD) relative to the catalytic domain of S1 (Fig. 6 *c*). This extends earlier studies by Garrigos et al. (1992) and Wakabayashi et al. (1992), who used models of the approximate shape of S1 to investigate such changes.

By use of the program MIDAS (Ferrin et al., 1988) we have, in the first instance, made torsional rotations about various C_α-C_α chords in the β-strand extending from Gln^{173} to Gly^{179} and lying near the bottom of the nucleotide cleft. We have used the 171–172, 173–174, 174–175, and 179–180 C_α-C_α chords, each of which makes somewhat different angles to the long axis of the β-strand, and have rotated all residues from the ends of these chords to residue 670. We believe these are plausible and representative ways of closing the jaws of the nucleotide pocket. In the second instance, we have torsionally rotated the entire LCBD about the C_α-C_α chord between residues 766 and 767 to move the LCBD (α-helix) axis toward the nucleotide pocket. A similar rotation was also made about the 705–706 region, which is located in the helix between the cross-linkable SH1 and SH2 thiols (693 and 707, respectively). Nucleotide trapping as a result of this cross-linking suggests that this region is implicated in the conformational change required for force production (Wells and Yount, 1982).

Fig. 7 shows the results of such rotations. There is a very strong dependence of R_g with angle for LCBD rotations but a much weaker dependence of R_g on nucleotide cleft-closing rotations of residues 172–670, etc. Using C_α van der Waal's radii we find that cleft closures are complete within less than 15°. This produces R_g changes of less than −1.5% (Fig. 7). Thus such cleft closures alone cannot account for

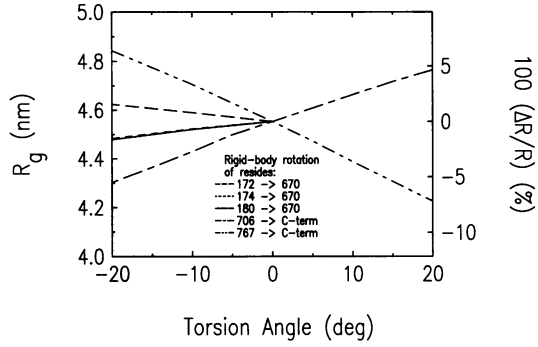

FIGURE 7 The expected change in R_gs for representative rigid-body rotations (see Fig. 6) as a function of torsion angle. Nucleotide-cleft closing torsional rotations were applied around the following (β-strand) C_α-C_α chords as follows: 171–172 (– – –) 173–174 (- - - -), 179–180 (——). Here all residues from the ends of these chords up to residue 670 were rotated as a single unit. Complete closure of the cleft occurred for rotations of less than 15°. LCBD torsional rotations around either the 705–706 (– - –) or the 766–767 C_α-C_α chords (– - - –) rotated this region toward the nucleotide cleft. Note that LCBD rotations produce much larger changes in R_g than do nucleotide-cleft closing rotations. The former are thus more consistent with the available data. Rotations of LCBD in both directions have been included to allow assessment of the maximum distortion possible between crystal and solution structures.

the change seen on addition of ATP (−6 ± 0.8%) (Wakabayashi et al., 1992) or of MgADP·V_i (−3.7 ± 0.8%) (average of neutrons and x-rays). This surprising result suggests that it is not simple nucleotide cleft closure alone that is directly responsible for the observed changes in R_g but rather movement about a more distal axis or a more complex movement of domains.

DISCUSSION

Amino acid analysis and enzymatic activity measurements indicate that the reductively methylated S1 produced in the current study is similar to that used in the crystal structure determination of S1 (Rayment et al., 1993a). Thus the results of this study can be compared to those of Rayment et al. with confidence.

The lack of change in R_g with methylation, with or without sulfate ion addition, is in concert with these alterations not inducing large-scale changes in the overall structure of S1. The alterations in ATPase activity (by methylation alone) seen here and by others seem to originate from local structural changes that do not induce global changes in S1 structure. The R_g is sensitive to the LCBD structure, as evidenced by the change in R_g of S1 seen when LC2 is not present (Mendelson et al., 1991; Garrigos et al., 1992) and to the orientation of LCBD relative to the remainder of S1. Thus the present results indicate that methylation (or methylation plus SO_4^{2-} ion) affects neither of these significantly. These results complement the crystallographic work on the catalytic domain of *Dictyostelium discoideum* myosin bearing bound ADP·BeF_x (I. Rayment, University of Wisconsin, 1994, personal communication), wherein it was shown that

this domain had a strong structural homology with the catalytic portion of vertebrate S1. The lack of change in structure on methylation is also suggested by the approximate structural homology between the unmethylated crystallographic structure of isolated LCBD (Protein Data Bank file *1scm*) from scallop (Xie et al., 1994) and intact LCBD in (methylated) chicken S1 (R. Mendelson, unpublished observations; see also Xie et al., 1994, and Bagshaw and Sutcliffe, 1994).

The relative resistance of the methylated S1 to proteolytic attack observed in the present study may result from the inability of proteases to attack peptide bonds involving methylated lysine residues or from stabilization of S1 to denaturation that may precede proteolysis. It is known that dimethyllysine residues in proteins are not cleaved by trypsin at a significant rate, whereas reductive methylation of trypsin itself does not reduce its catalytic activity (Means, 1977). Although Phan et al. (1994) reported increased susceptibility to heat denaturation after methylation of S1, reductive alkylation has been reported to stabilize chymotrypsinogen A (Fujita and Noda, 1991) and glycogen phosphorylase b (Shatsky et al., 1973) to denaturation, possibly by increasing the hydrophobicity of lysine ϵ-amino groups. Resistance to proteolysis may have been a contributing factor in the successful crystallization of reductively methylated S1.

Although methylation does not change R_g, we find [in agreement with the results of Wakabayashi et al. (1992)] that ADP·V_i addition does. In the Wakabayashi et al. work, the slopes of the concentration dependencies of S1·ADP·V_i and free S1 are the same, but they are different from S1 plus ATP and also from our (and Garrigos et al., 1992) nucleotide-free S1 concentration dependence. Although the origin of the difference in these dependencies is unclear and could conceivably be statistical, it is nevertheless reassuring that on addition of ADP·V_i our $\Delta R_g^{eff}/R_g^{eff}$ is identical with theirs within error.

Comparison of nucleotide-free neutron data with those expected from the crystal structure suggests that the experimental R_g is close to, but not identical to, that predicted by the crystal structure. Some of the (~3%) increase in the scattering R_g over the crystal R_g may be due to a change in S1 shape such as a pivoting of the LCBD (<20°; see Fig. 7). Such a difference could result from strain induced as a result of crystallization. Other possibilities may, in principle, account for some or all of this difference. Most of the preparations used in the scattering experiments contained about 20–40% of (enzymatically clipped) LC1, which contains an additional 2–3 kDa of unknown structure. The 19 NH_2—terminal residues of LC2, which are absent in the crystal structure, could have a structure that deviates significantly from our "point" approximation, or a small amount of undetected residual aggregation might be significant. In addition, a small increase of the experimental R_g over that calculated from $R_g^{in\ vacuo}$ is also expected to arise from bound surface water molecules that extend the boundary between protein and bulk solvent beyond the confines of the S1 van der Waal's envelope. However, the sparse and incomplete structural information currently available on the protein-water interface inhibits accurate model-building efforts. Thus, although a small decrease in R_g could be occurring upon crystallization, the overall crystallographic shape could well be identical to that in solution. We are currently investigating this issue further by analysis of high-angle x-ray scattering data.

We find good agreement between the solution x-ray scattering results of Garrigos et al. (1992) and our neutron scattering results; the nucleotide-free R_g^{eff} found by Wakabayashi et al. (1992) is somewhat larger. This may be related in part to differences in concentration dependencies of the R_g of nucleotide-free S1.

We have found that simple closure of the nucleotide cleft by rotation about an axis along its base alone cannot explain the observed changes in R_g on nucleotide addition. Although this seems to be in serious disagreement with the simplest form of the model set out by Rayment et al. (1993b), we cannot exclude more complex closures of this cleft with certainty. However, another possibility is a rotation of the LCBD of S1, which could readily produce such changes. It is interesting to note that a torsional rotation of 5–15° about the 705–706 C_α-C_α chord or the 766–767 C_α-C_α chord would bring the residue 105–114 α-helix of LC3 into close proximity with the residue 21–29 α-helix of the heavy chain. We speculate that such an interaction could play a role in myosin-linked regulation of certain mollusks (Szent-Györgyi et al., 1973). If the scallop heavy chain possesses a similar NH_2-terminal structure, a path for communication would exist from the (regulatory) Ca^{2+} binding site on the essential light chain (LC1 or LC3 in vertebrates) to the nucleotide site.

Note: Subsequent to the submission of this manuscript, a preliminary account of the crystallographic structures of *D. discoideum* catalytic domains (S1Dc) (which are devoid of the LCBD) with bound MgADP·BeF_x and MgADP·AlF_4 was reported (Fisher et al., 1995). The results of this work are in harmony with the conclusions of the present work. As discussed earlier, no major structural differences between S1Dc·MgADP·BeF_x and the equivalent portion of intact methylated chicken S1 were found. In addition, no significant changes in the degree of closure of the nucleotide pocket by these nucleotide analogs was detected. The solvent accessibility of fluorescent nucleotides bound to S1 does not seem to change, which also suggests that nucleotide cleft closure is not significant during ATP hydrolysis (Franks-Skiba and Cooke, 1995)

We thank Dr. Ivan Rayment for helpful conversations and for furnishing the crystallographic structure of S1. We are grateful to Drs. Charles Glinka and Susan Kreuger of the National Institute of Science and Technology (Gaithersburg, MD) for assistance and advice during data collection. We thank Dr. Peter Timmins for helpful discussions. We acknowledge the able technical assistance of Ms. Racquel Tagunicar.

The experiments were performed on the basis of activities supported by the National Science Foundation under Agreement DMR-9122444 (NIST).

This work was conducted at facilities supported by the Departments of Energy and Commerce. We acknowledge the use of the UCSF Computer Graphics Laboratory, which is supported by National Institutes of Health National Center for Research Resources RR-01081.

This work was supported in part by National Institutes of Health Grants R01-AR39710 and P01-AR42895 to Robert A. Mendelson.

REFERENCES

Aguirre, R., F. Gonsoulin, and H. C. Cheung. 1986. Interaction of fluorescently labeled myosin subfragment 1 with nucleotides and actin. *Biochemistry.* 25:6827–6835.

Bagshaw, C. R., and M. J. Sutcliffe. 1994. Another turn for E-F hands. *Nature Struct. Biol.* 1:209–212.

Bivin, D. B., K. Ue, M. Khoroshev, and M. F. Morales. Effect of lysine methylation and other ATPase modulators on the active site of myosin subfragment 1. *Proc. Natl. Acad. Sci. USA.* 91:8665–8669.

Ferrin, T. E., C. C. Huang, L. E. Jarvis, and R. Langridge. 1988. The MIDAS display system. *J. Mol. Graphics.* 6:13–27.

Fisher, A., C. A. Smith, J. Thoden, R. Smith, K. Sutoh, H. M. Holden, and I. Rayment. 1995. Structural studies of myosin:nucleotide complexes: a revised model for the molecular basis of muscle contraction. *Biophys. J.* 68:19s–28s.

Franks-Skiba, K., and R. Cooke. 1995. The conformation of the active site of myosin probed using mant-nucleotides. *Biophys. J.* 68: 142s–149s.

Fretheim, K., S. Iwai, and R. E. Feeney. 1979. Extensive modification of protein amino groups by reductive addition of different sized substituents. *Int. J. Pept. Protein Res.* 14:451–456.

Fujita, Y., and Y. Noda. 1991. Effect of reductive alkylation on thermal stability of ribonuclease A and chymotrypsinogen A. *Int. J. Pept. Protein Res.* 38:445–452.

Garrigos, M., S. Mallam, P. Vachette, and J. Bordas. 1992. Structure of the myosin head in solution and the effect of light chain 2 removal. *Biophys. J.* 63:1462–1470.

Goodno, C. C. 1982. Myosin active-site trapping with vanadate ion. *Methods Enzymol.* 85:116–123.

Goodno, C. C., and E. W. Taylor. 1982. Inhibition of actomyosin ATPase by vanadate. *Proc. Natl. Acad. Sci. USA.* 79:21–25.

Huang, Z., J. M. Gabriel, M. A. Baldwin, R. J. Fletterick, S. B. Prusiner, and F. E. Cohen. 1994. Proposed three-dimensional structure for the cellular prion protein. *Proc. Natl. Acad. Sci. USA.* 91:7139–7143.

Ibel, K., and H. B. Stuhrmann. 1979. Comparison of neutron and x-ray scattering of dilute myoglobin solutions. *J. Mol. Biol* 93:255–265.

Jacrot, B., and G. Zaccai. 1981. Determination of molecular weight by neutron scattering. *Biopolymers.* 20:2413–2426.

Kitagawa, S., J. Yoshimura, and Y. Tonomura. 1961. On the active site of myosin A-adenosine triphosphatase. *J. Biol. Chem.* 236:902–906.

Kraulis, P. J. 1991. MOLSCRIPT: a program to produce both detailed and schematic plots of protein structures. *J. Appl. Cryst.* 24:946–950 .

Margossian, S. S., and S. Lowey. 1982. Preparation of myosin and its subfragments from rabbit skeletal muscle. *Methods Enzymol.* 85:55–72.

Means, G. E. 1977. Reductive alkylation of amino groups. *Methods Enzymol.* 47:469–478.

Mendelson, R. A., D. Bivin, P. M. G. Curmi, D. K. Schneider, and D. B. Stone. 1991. Recent neutron scattering studies of muscle contraction and its control. *Adv. Biophys.* 27:143–153.

Moore, P. B. 1980. Small-angle scattering. Information content and error analysis. *J. Appl. Cryst.* 14:168–175.

Muhlrad, A., Y. M. Peyser, and I. Ringel. 1991. Effects of ions on vanadate-induced photocleavage of myosin subfragment 1. *Eur. J. Biochem.* 201:409–415.

Phan, B. C., P. Cheung, C. J. Miller, E. Reisler, and A. Muhlrad. 1994. Extensively methylated myosin subfragment-1: examination of local structure, interactions with nucleotides and actin and ligand-induced conformational changes. *Biochemistry.* 33:11286–11295.

Rayment, I., W. R. Rypniewski, K. Schmidt-Bäse, R. Smith, D. R. Tomchick, M. M. Benning, D. A. Winkelmann, G. Wesenberg, and H. M. Holden. 1993a. Three-dimensional structure of myosin subfragment-1: a molecular motor. *Science.* 261:50–58.

Rayment, I., H. M. Holden, M. Whittaker, C. B. Yohn, M. Lorenz, K. C. Holmes, and R. A. Milligan. 1993b. Structure of the actin-myosin complex and it implications for muscle contraction. *Science.* 261:58–65.

Ring, C. S., D. G. Kneller, R. L. Langridge, and F. E. Cohen. 1992. Taxonomy and conformational analysis of loops in proteins. *J. Mol. Biol.* 224:685–699.

Rypniewski, W. R., H. M. Holden, and I. R. Rayment. 1993. Structural consequences of reductive methylation of lysine residues in hen egg white lysozyme: an x-ray analysis at 1.8-Å resolution. *Biochemistry.* 32:9851–9858.

Schoenborn, B. 1975. Advantages of neutron scattering for biological structure analysis. *In* Neutron Scattering for the Analysis of Biological Structures. B. Schoenborn, editor. Brookhaven National Laboratory, Upton, New York. I10–I17.

Shatsky, M. A., H. C. Ho, and J. H.-C. Wang. 1973. Stabilization of glycogen phosphorylase *b* by reductive alkylation with aliphatic aldehydes. *Biochem. Biophys. Acta.* 303:298–307.

Smith, S. J., and E. Eisenberg. 1990. A comparison of the effect of vanadate on the binding of myosin-subfragment-1 ADP to actin and on actomyosin subfragment 1 ATPase activity. *Eur. J. Biochem.* 193: 69–73.

Spudich, J. A., and S. Watt. 1971. The regulation of rabbit skeletal muscle contraction. I. Biochemical studies of the interaction of the tropomyosin-troponin complex with actin and the proteolytic fragments of myosin. *J. Biol. Chem.* 239:2360–2364.

Szent-Györgyi, A. G., E. M. Szentkiralyi, and J. Kendrick-Jones. 1973. The light chains of scallop myosin as regulatory subunits. *J. Mol. Biol.* 74:179–203.

Takashi, R., A. Muhlrad, and J. Botts. 1982. Spatial relationship between a fast-reacting thiol and a reactive lysine residue of myosin subfragment 1. *Biochemistry.* 21:5661–5668.

Tesi, C., T. Barman, and F. Travers. 1988. Sulfate is a competitive inhibitor of the binding of nucleotide to myosin. A comparison with phosphate. *FEBS Lett.* 236:256–260.

Toyoshima, Y. Y., S. J. Kron, E. M. McNally, K. R. Niebling, C. Toyoshima, and J. A. Spudich. 1987. Myosin subfragment-1 is sufficient to move actin filaments in vitro. *Nature.* 328:536–539.

Tsai, C. S., Y.-H. Tsai, G. Lauzon, and S. T. Cheng. 1974. Structure and activity of methylated horse liver alcohol dehydrogenase. *Biochemistry.* 13:440–443.

Vibert, P., and C. Cohen. 1988. Domains, motions and regulation in the myosin head. *J. Muscle Res. Cell Motil.* 9:296–305.

Wakabayashi, K., M. Tokunaga, I. Kohno, Y. Sugimoto, T. Hamanaka, Y. Takezawa, T. Wakabayashi, and Y. Amemiya. 1992. Small-angle synchrotron x-ray scattering reveals distinct shape changes of the myosin head during hydrolysis of ATP. *Science.* 258:443–447.

Wells, J., and R. Yount. 1982. Chemical modification of myosin by active-site trapping of metal-nucleotides with thiol crosslinking reagents. *Methods Enzymol.* 85:93–116.

White, H. D. 1982. Special instrumentation and techniques for kinetic studies of contractile systems. *Methods Enzymol.* 85:698–708.

White, H. D., and I. Rayment. 1993. Kinetic characterization of reductively methylated myosin subfragment 1. *Biochemistry.* 32:9859–9865.

Xie, X., D. H. Harrison, I. Schlichting, R. M. Sweet, V. N. Kalabokis, A. G. Szentz-Györgyi, and C. Cohen. 1994. Structure of the regulatory domain of scallop myosin at 2.8 Å resolution. *Nature.* 368:306–312.